# Microstructure fiber-tip sensor with spectral encoding

P. Sixt, L. Falco, P. Dierauer*, H.W Lehmann+

Centre Suisse d'Electronique et de Microtechnique S.A. - Recherche et Développement -
Maladière 71, 2000 Neuchâtel 7, Switzerland
* Engineer School, Biel, Switzerland
+ Paul Scherrer Institute, 8048 Zürich, Switzerland

## ABSTRACT

Two of the main practical difficulties met by fibre point sensors where the measurand acts on the optical signal by means of a membrane or a cantilever are on one hand the thermal and mechanical stability as well as the vulnerability, and, on the other hand, the optical power referencing.

Both problems have been solved here by designing a monolithic low order reflection Fabry-Perot microstructure using fibre tip dielectric and metallic mirrors. The suitably designed optical transfer function of the Fabry-Perot can easily be separated from the transfer function of the multimode fibre lead within the optical bandwidth of a cheap light emitting diode. This approach lends itself to batch fabrication and assembling with sensitivity and dynamic range adjustable by controlling the geometrical and technological parameters of planar photolithographic techniques and etching processes.

A pressure sensor with 128 resolvable points within a 30 nm spectral width centered at 830 nm is described.

## 1. INTRODUCTION

Extrinsic fiber optic point sensors in which the fiber is only used as a lead to and from a mechanical structure transducing the variation of a physical quantity into light intensity modulation have numerous simple applications. However, they suffer from a number of practical difficulties due to their hybrid nature: sensitivity to vibration and, more generally, to environmental conditions, low mechanical bandwidth, temperature vulnerability and instability, low accuracy, low material but high assembling and packaging costs. There is another, more fundamental, difficulty in that the intensity modulated optical signal returning from the transducer cannot be separated from intensity fluctuations of the source and on the fiber lead.

It has long been recognized that spectral encoding is well suited to fiber sensors as the fiber, if multimode, can be considered as achromatic relative to splice, connector, bending and microbending losses. The encoding for the aforementioned mechanical structures involving membranes or cantilevers can very well be performed by using a fiber-end Fabry-Pérot configuration[1,2]. If, in addition, the interferometer is a low-order Fabry-Pérot placed in the fiber near-field region without collimation optics, the whole transducer assembly can then become monolithic, rugged and small-size, and lend itself to inorganic bonding[3].

A fiber-tip low-order Fabry-Pérot microstructure will be used here as a pressure sensor. The whole transducer head has been achieved in glass in order to limit the effects of temperature expansion coefficient differentials.

## 2. THEORETICAL ANALYSIS

### 2.1. Optical modelisation of the cavity

2.1.1. Plane wave. When a plane monochromatic wave propagating in a medium of index n falls on a cavity determined by two plane parallel interfaces separated by a distance e, delimiting a transparent medium of index n', the reflected power is modulated by the well-known Airy function[4]:

$$I_r = I_0 \frac{F \sin^2 \frac{\delta}{2}}{1 + F \sin^2 \frac{\delta}{2}} \quad (1)$$

where:

$$\delta = \frac{4\pi}{\lambda} n' e \cos\theta \quad \text{is one round trip phaseshift in the cavity.} \quad (2)$$

$$F = \frac{4\,\mathbf{R}}{(1 - \mathbf{R})^2} \quad \text{where } \mathbf{R} = \left(\frac{n - n'}{n + n'}\right)^2 \text{ is the power reflection coefficient of a single mirror} \quad (3)$$

For low values of **R**, the function $I_r(\delta)$ is approximately sinusoïdal, but as **R** approaches unity, $I_r$ exhibits sharp minima for integer values m of $(\delta/2\pi)$, as illustrated in Fig. 1, m being the order of the cavity.
The width of the peaks at half maximum reflected power, i.e. the finesse **F** of the cavity, is related to the F parameter by:

$$\mathbf{F} = \pi \frac{F^{1/2}}{2} . \quad (4)$$

In a balanced cavity, the finesse increases with increasing **R**.
The spectral position of the minima of $I_r$ is given by $\lambda = 2\frac{d}{m}$. (5)
($d = n' e \cos\theta$ being the optical length of the cavity).

This illustrates the necessity of working with a low-order cavity in a sensor system where the detected physical quantity is the position $\lambda_0$ of the reflected power minima under a variation of d, to get a high enough sensitivity.

In an unbalanced Fabry-Pérot (with differing mirror reflectivities), the modulation depth is notably lowered: as the destructive interference is not total, the minimum reflected power is not zero and the new contrast factor is:

$$\frac{I_{max}}{I_{min}} = \left(\frac{r' + r''}{r' - r''}\right)^2 \cdot \left(\frac{1 - r'r''}{1 + r'r''}\right)^2 \quad \text{, where } r' \text{ and } r'' \text{ are the two field coefficients} \quad (6)$$

This sensor works in the reflection mode with a metal end-mirror in order to prevent light from leaking into the medium in which sensing occurs and to isolate the transducer's optical transfer function from ambient optical radiation. A metallic mirror provides optical isolation while still allowing not too high a finesse to be achieved so that the read out of the spectral response of the Fabry-Pérot can be performed by rather simple means. Using a metal mirror offers further interesting features left aside in the present application, e.g. efficient optical powering[5], efficient local excitation of surface non-linear effects.

2.1.2. Monomode fiber To estimate the limitations on the performances of an end-fiber Fabry-Pérot type sensor, it is necessary to introduce a model more adapted to the geometry of the problem than the plane wave hypothesis.

The case of a monomode fiber will first be considered; although in practice a multimode fiber based system has much more potential applications (mainly because of the lower cost of components, larger tolerances and higher injected power), the monomode case represents a good basis for discussing the influences of fiber-cavity distance and cavity width, in an ideal case where the ultimate performances of the system can more easily be evaluated.

The field on the end face of a single-mode fiber can be considered Gaussian with a very good approximation[6], except in the region far from the core-cladding interface, where it decreases exponentially.

$$\psi = \psi_0 \exp\left[-\left(\frac{r}{w_0}\right)^2\right] \tag{7}$$

Moreover, in the weak guidance hypothesis, transverse components of the field are dominant and the scalar approximation can be used. The propagation of the field through free space can be studied either with the scalar diffraction theory (starting with the Kirchhoff integral, then using paraxial and Fresnel approximations), or with a simplified form of the scalar wave equation. In each case, the solution is found to be the well-known Gaussian beam[7]:

$$\psi(x,y,z) = \frac{w_0}{w(z)}\,\psi_0 \exp\left[-j\left(kz + \frac{\pi r^2}{\lambda R(z)} + \arctan\left(\frac{\lambda z}{\pi w_0{}^2}\right)\right)\right] \cdot \exp\left(-\frac{r^2}{w^2}\right) \tag{8}$$

where:

$$w(z) = w_0\left[1 + \left(\frac{\lambda z}{\pi w_0{}^2}\right)^2\right]^{1/2} \quad \text{is the beam waist at distance } z \tag{9}$$

$$R(z) = z\left[1 + \left(\frac{\pi w_0{}^2}{\lambda z}\right)^2\right] \quad \text{is the radius of curvature of the wave} \tag{10}$$

Between two plane parallel mirrors, no stable Gaussian mode exists, so the beam widens as it travels back and forth across the cavity. Provided no distorsion of the beam exists at the reflection on the mirrors (that is not completely true for the outer components of the transverse spatial spectrum reflecting on a multilayer dielectric mirror), the reflected power can be expressed as:

$$I_r = \left| \sum_{i=0}^{\infty} 2\,\frac{w_0}{w(z_i)}\,c_i\,\frac{\exp\left[-j\left(kz_i - \arctan\left(\frac{\lambda z_i}{\pi w_0{}^2}\right)\right)\right]}{\left[1 + \left(\frac{w_0}{w(z_i)}\right)^2 + j\,\frac{\pi w_0{}^2}{\lambda R(z_i)}\right]} \right| \tag{11}$$

with: $z_i = 2(y + ie)$ (y is the fiber end - resonator distance)
$c_0 = r$
$c_i = tt'r'^{2i-1}$ $(i \geq 1)$

Using this expression for $I_r$, the finesse of the cavity has been calculated when the cavity is directly in front of the fiber (Fig. 2.a)) or at a distance of 50 $\mu$m (Fig. 2.b)). In both cases, the cavity is used at the fourth order (e = 1.4 $\mu$m at $\lambda$ = 820 nm), with mirror reflectivity R = R' = 0.85, giving a theoretical maximum finesse of $\simeq$ 19.5.

In the Gaussian beam the minimum radius of curvature of the wave surface (i.e. the point where the beam differs most from a plane wave, or where its angular dispersion is the highest) occurs for:

$$z = \frac{\pi w_0{}^2}{\lambda} \tag{12}$$

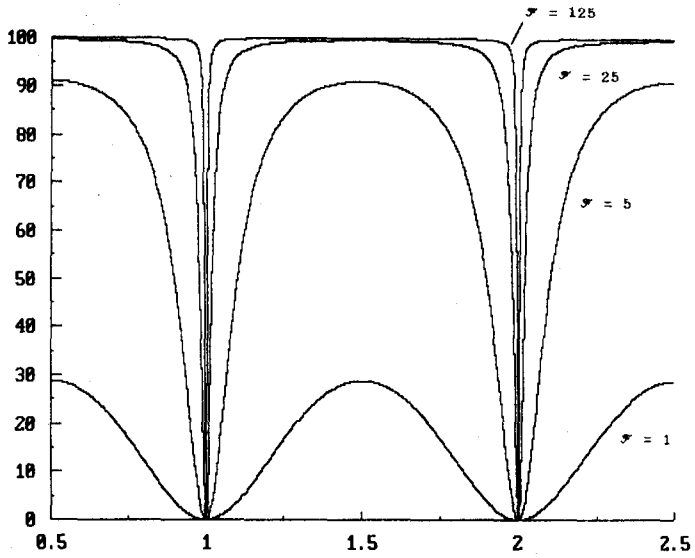


Figure 1.

Theoretical spectral caracteristic of plane-wave Fabry-Pérot: reflected power $I_r$ versus cavity order ($\delta/2\pi$) with various finesse values.

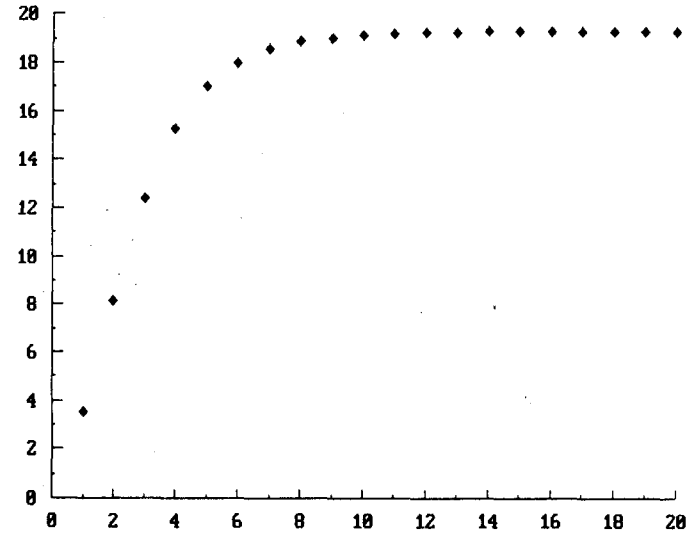


Figure 2.a)

Theoretical finesse of a monomode fiber-end Fabry-Pérot versus spot diameter $2w_0$ in microns (wavelength: $\lambda$ = 820 nm, cavity width: e = 1.4 $\mu$m, fiber-cavity longitudinal distance: y = 0 $\mu$m, mirror reflectivity: R = R' =0.85)

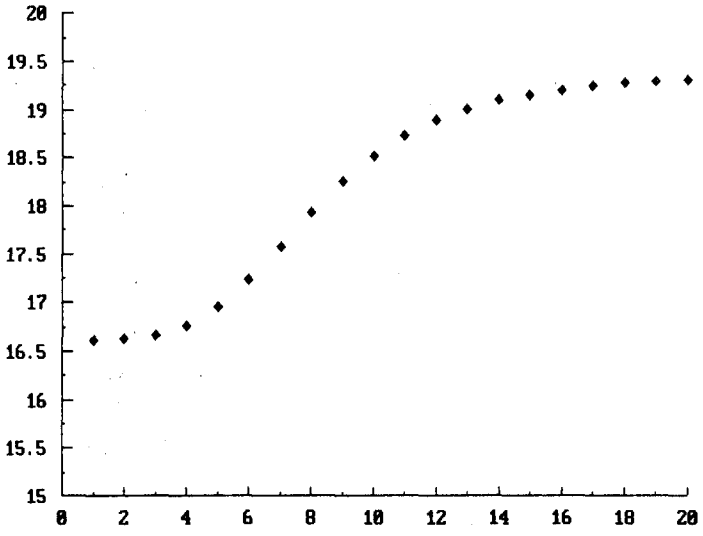


Figure 2.b)

Same but with fiber-cavity distance: y = 50 $\mu$m

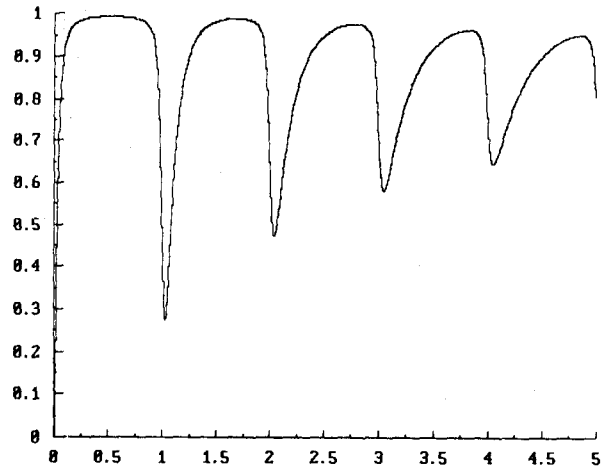


Figure 3.a)

Theoretical reflected power $I_r$ in a low-order monomode fiber-end Fabry-Pérot versus cavity order ($\delta/2\pi$) (here: variable cavity width; wavelength: $\lambda$ = 820 nm, fiber spot diameter: 1 $\mu$m, fiber-cavity longitudinal distance: y = 0 $\mu$m, mirror reflectivity: R = R' = 0.85)

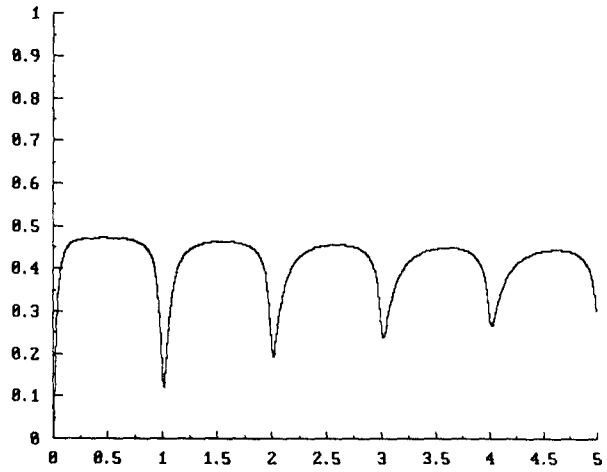


Figure 3.b)

Same but with fiber-cavity longitudinal distance: y = 1 $\mu$m

This explains the strong dependance of the finesse on the spot radius $w_0$, observed in Fig. 2.a): with a small $w_0$, the first interfering beams are strongly affected, while with the $w_0$ of standard fibers (4 to 5 $\mu$m), only the smaller terms of the interference sum are modified; the finesse is thus practically the same as in the case of a plane wave. By comparison, when the cavity is further away from the fiber end, the cavity is already in the far field of the beam, especially with a low $w_0$, so the finesse is also much higher (a 100% increase, for example, with $w_0$ = 2$\mu$m); however, in this case, the insertion loss is also higher. Fig. 3.a) and b) show the reflected power for $w_0$ = 1 $\mu$m, with a cavity located respectively at 0 and 1 $\mu$m from the fiber end; it illustrates the widening and deformation of the peaks when e increases (due to the higher angular dispersion) and the higher insertion loss but also higher finesse when the cavity is further away.

In conclusion, for a standard monomode fiber, the finesse is not significantly affected by the guided-wave effects, and the cavity can be placed some distance away from the fiber end, the only limiting factor being the insertion loss.

2.1.3 Multimode fiber. With a multimode fiber, two effects could lead to a deterioration of the finesse of the cavity: the retrocoupling loss suffered by the beam during one cavity round trip, and the indetermination on the optical length of the cavity, due to modal dispersion; in a low-order Fabry-Pérot, the latter is by far the most important; using the approached expression of the coupling coefficient $\eta$ between two identical fibers[8]: $\eta \simeq 1 - 0.33\ N\zeta$, with $\zeta = z/a$ (N: numerical aperture, z: inter-fiber distance, a: fiber core radius), and for a cavity with e = 1.4 $\mu$m, we find a loss $\eta \simeq 0.98$, i.e. a reduction factor of $\simeq 0.87$ on the finesse.

The second effect has been estimated, with a planar model, supposing uniform excitation of all modes (a very pessimistic hypothesis!); a 40% decrease of the finesse results, with a fiber of 0.2 NA. This decrease in itself is not critical, because one could use highly reflecting mirrors, giving a high initial finesse; far more serious could be the fluctuations of the modal distribution, that can lead to an indetermination on the position of the peaks, and so to a decrease of the overall accuracy. However, these fluctuations are second-order effects; they act indirectly on the optical path length, which is proportional to the cosine of the ray angle $\theta$. Moreover, it seems reasonable to suppose the widening around the minima to be symmetrical with respect to the center of the peaks. An appropriate detection system, with a large number of spectral points to determine the position of the minima, enabling a curve-fitting to be performed, should therefore eliminate this problem.

The influence of the longitudinal position of the cavity with respect to the fiber end should be much the same than in the monomode case: the most important effect is a greater insertion loss, with nearly no influence on the finesse, this loss acting identically on the different interfering contributions.

## 2.2. Mechanical configuration

The deformation of a thin circular membrane fixed on its periphery, under a uniform differential pressure $\Delta P$, is given by[9]:

$$\Delta z = \frac{3R^4}{16e^3} (1 - \nu^2) \frac{\Delta P}{E} \qquad (13)$$

with:

E: Young's modulus
$\nu$: Poisson ratio
R: membrane radius
e: membrane thickness

It is important to note that in the case of a membrane simply supported on its periphery, this expression is multiplied by the factor $f = (5 + \nu)/(1 + \nu)$, which in the case of the glass we used is about 4.3: this shows the crucial importance of the membrane bonding technology.

The other point is the sensitivity of the system to the dimensional parameters R and e. To give a practical example of pressure sensor, the deformation of a membrane with R = 0.5 mm and e = 50 $\mu$m (thinnest commercially available glass) is about 120 nm/bar; in a medium pressure range of 0 - 1 bar, with a spectral sensitivity factor of 0.4 (cf. § 3.), this value is optimal for covering the whole 3 dB spectrum of a common LED. Similarly, a 250 $\mu$m membrane could be used for high pressures (0 - 100 bar), or a 10 $\mu$m membrane for very low pressures (0 - 10 mbar).

One of the advantages of this type of sensor is its self-protecting effect: in case of overpressure, the membrane touches the other side of the cavity and is therefore mechanically protected; with the 50 $\mu$m membrane and a 1.4 $\mu$m cavity, this phenomenon only occurs for a 1000% overpressure, and without significant mechanical stress, the diameter/deformation ratio being about 1000. The resonant frequency of such a small membrane is extremely high: $f_{res} \simeq 660$ kHz with the above values (R = 0.5 mm, e = 50 $\mu$m); in practice, the bandwidth limitations come from the electronics rather than from the membrane. An advantage of this high frequency is the very good insensitivity of the sensor against external vibrations. Also, the very small volume of the sensor introduces practically little perturbation in the physical system being investigated.

## 3. EXPERIMENTAL RESULTS

To get rid of the fluctuations of the reflected power $I_r$, due to the source and to loss variations on the lead to the transducer, the method generally applied with Fabry-Pérot cavities excited by wide spectrum sources is the measurement of $I_r$ at two different wavelengths[3]; this also enables the determination of the sign of the membrane displacement to be performed.

The present system determines the position of the reflected power minima in the spectral range of a wide band source. This approach requires a more complex optical hardware such as a dedicated spectrometer. The use of CCD and A/D conversion limits the overall sensor bandwidth. However, better referencing can be achieved regarding wavelength dependent perturbations such as fiber bending and coupling loss and, more importantly, temperature change and ageing of the semiconductor source. These effects are smoothly wavelength dependent and their presence will not significantly perturb the overall spectral response of the transducer. In particular, the position of the minima will be practically unaffected. The ambiguity on the determination of $\Delta e$ also disappears, even if more than one minimum is present at the same time in the detected spectrum, provided the shift does not exceed one free spectral range.

If there is no wavelength dependence of the optical medium within the cavity, the shift of the minima is linear with respect to the mirror displacement, with:

$$\Delta \lambda_{min} = \frac{2}{m - \frac{\phi}{2\pi}} \Delta e \qquad (14)$$

Figure 4.

Fabry-Pérot pressure sensor detection system

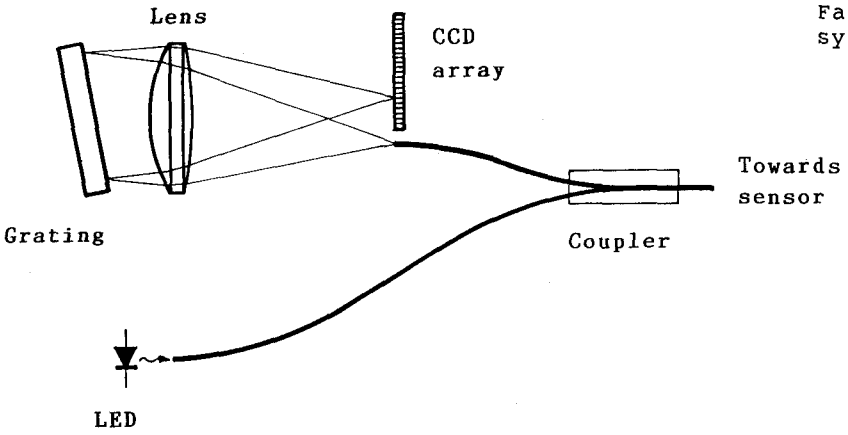


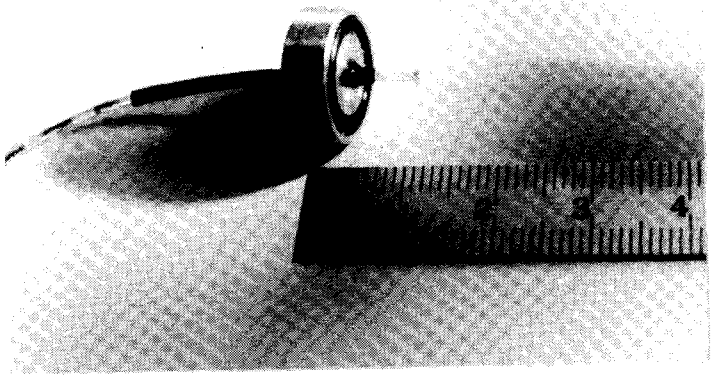

Figure 5.

Optical head of pressure sensor prototype.

Where $\phi$ is the phase change at the reflection on the mirrors ($\phi \simeq 192°$ for aluminium at 820 nm). In case a dielectric mirror is used on the fiber side of the cavity, this phase change $\phi(\lambda)$ can be as high as $\pm$ 40° for $\Delta\lambda$ = 100 nm; this mainly results in a modification of the optical sensitivity $s = \Delta\lambda_{min}/\Delta e$ for a given order m. The present system uses a multilayer dielectric mirror[10]. A sensitivity $s \simeq 0.38$ was obtained. This can be compared to the figure of 0.58 that was expected from the design where a wavelength independent reflection coefficient was attributed to the first mirror.

The detection system represented in Fig. 4. was dimensioned to scan a spectrum of 30 nm centered at $\lambda$ = 820 nm; this corresponds to the present geometry of the membrane (R = 0.89 mm, $\Delta z$ = 50 $\mu$m, giving a mechanical sensitivity of 77 nm/bar) and of the membrane (e = 1.4 $\mu$m, giving an optical sensitivity of 0.38 nm/nm) for a 0 - 1 bar pressure measurement range. Fig. 5. shows a terminated sensor head prototype.

A grating with 1200 lines/mm blazed at 750 nm, mounted in a Littrow position, and a 128 element CCD were used in a dedicated spectrometer.

The first experiments, performed with membranes organically bonded at their periphery, proved the feasability of the approach. Fig. 6. shows a curve-fitting performed on the central portion of a spectrum transferred on a PC via a fast A/D card.

Membrane displacements and peak widths larger than predicted were observed as well as hysteresis; these undesirable features are being notably reduced with non-organic bonding technology.

The present efforts are mainly centered on new glass to glass and metal to glass bonding techniques; thermodiffusion and anodic bonding[11] have already shown promising results that will be reported.

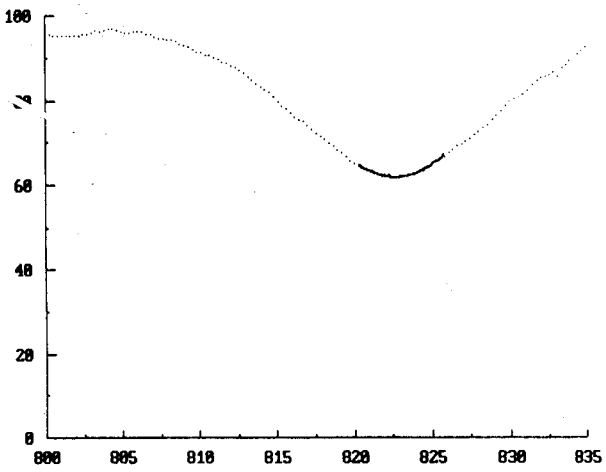


Figure 6.

Experimental 128-point detected spectrum with parabolic curve-fitting around a Fabry-Pérot minimum: reflection coefficient versus wavelength in nm.

## 4. ACKNOWLEDGMENTS

The authors are grateful to Mr H. Brunner, Paul Scherrer Inst., Zürich, for the deposition of the dielectric mirrors. They also thank Dr. O. Parriaux for his useful assistance.

## 5. REFERENCES

1. E.R. Cox, B.E. Jones, Fiber optic colour sensor based on Fabry-Pérot interferometry, Proc. 1st Int. Conf. on Opt. Fiber Sensors London, pp. 122-124 (1983)

2. J.P Dakin, C.A. Wade and P.B. Withers, An optical fiber pressure sensor, J. Opt. Sensors, vol.2, n°3, 191-199 (1987)

3. E.W. Saaski, J.C. Hartl, G.L. Mitchell, R.A. Wolthuis, M.A. Afromowitz, A family of fiber optic sensors using cavity resonator microshifts, Proc. OFS Tokyo, pp. 11-14 (1986)

4. M. Born and E. Wolf, Principles of Optics, Pergamon, Oxford (1980)

5. M. Johnson, Optical powering techniques for microstructure fiber sensors, IGI Europe, ed., Boston, MA, Proc. EFOC/LAN Amsterdam, 219-222 (1988)

6. D. Marcuse, Gaussian approximation of the fundamental modes of graded-index fibers, J. Opt. Soc. Am., vol.68, n°1, pp. 103-109 (1978)

7. D. Marcuse, Light Transmission Optics, Van Nostrand Reinhold, New York (1982)

8. W. van Etten, W. Lambo, P. Simons, Loss in multimode fiber connections with a gap, Appl. Opt., vol. 24, n°7, pp. 970-976 (1985)

9. S.P. Timoshenko, Résistance des matériaux, t.2, Dunod, Paris (1968)

10. M.T. Gale, H.W. Lehmann, In-situ optical monitoring of thin films during evaporation, Proc. SPIE Hamburg, Paper Nr 1019-12 (1988)

11. G. Wallis, D.I. Pomerantz, Field-assisted glass-metal sealing, J. Appl. Physics, vol. 40, n°10, pp. 3946-3949 (1969)